Published online 4 April 2018

Nucleic Acids Research, 2018, Vol. 46, No. 8 ***3833–3840***
doi: 10.1093/nar/gky242

SURVEY AND SUMMARY

Structural dynamics of the N-terminal domain and the Switch loop of Prp8 during spliceosome assembly and activation

Xu Jia* **and Chengfu Sun***

Non-coding RNA and Drug Discovery Key Laboratory of Sichuan Province, Chengdu Medical College, Chengdu 610500, China

Received January 09, 2018; Revised March 02, 2018; Editorial Decision March 21, 2018; Accepted April 03, 2018

ABSTRACT

Precursor message RNA (pre-mRNA) splicing is executed by the spliceosome, a large ribonucleoprotein (RNP) machinery that is comparable to the ribosome. Driven by the rapid progress of cryo-electron microscopy (cryo-EM) technology, high resolution structures of the spliceosome in its different splicing stages have proliferated over the past three years, which has greatly facilitated the mechanistic understanding of pre-mRNA splicing. As the largest and most conserved protein in the spliceosome, Prp8 plays a pivotal role within this protein-directed ribozyme. Structure determination of different spliceosomal complexes has revealed intimate and dynamic interactions between Prp8 and catalytic RNAs as well as with other protein factors during splicing. Here we review the structural dynamics of two elements of Prp8, the N-terminal domain (N-domain) and the Switch loop, and delineate the dynamic organisation and underlying functional significance of these two elements during spliceosome assembly and activation. Further biochemical and structural dissections of idiographic splicing stages are much needed for a complete understanding of the spliceosome and pre-mRNA splicing.

INTRODUCTION

Pre-mRNA splicing, the process for removal of introns and ligation of exons, is catalysed by a mega-Dalton ribonucleoprotein (RNP) machinery, termed the spliceosome (1). The spliceosome consists of five small nuclear RNPs (snRNPs), each of which contains one piece of uridine-rich small nuclear RNA (snRNA) and several respective specific proteins, in addition to dozens of non-snRNP proteins. The process of pre-mRNA splicing generally is composed of four steps: assembly, activation, catalysis and disassembly, and is directed by eight consecutive spliceosomal complexes that have been characterised to date (Figure 1). The spliceosome is assembled first into the A complex, which is composed of U1 and U2 snRNPs and the substrate, a pre-mRNA intron, and then into the pre-catalytic B complex after recruiting the pre-formed U4/U6.U5 tri-snRNP. For catalysis to occur, the spliceosomal B complex needs to be activated into the B^{act} complex, a process involving dramatic conformational and compositional changes, and further catalytically activated into the B* complex as executed by an ATPase, Prp2. The spliceosomal B* complex in turn catalyses the first transesterification reaction of splicing, whereas the resultant C complex, after transformed into the C* complex by Prp16, catalyses the second transesterification reaction. After catalysis, the products, the mRNA and intron lariat, are released, and the spliceosome is disassembled and prepared for the next round of splicing.

High-resolution structure of the spliceosome is critical to the mechanistic understanding of pre-mRNA splicing. Through the substantial advancement of cryo-electron microscopy (cryo-EM) technology, the first atomic structure of the spliceosome was resolved in 2015 (2). Subsequently, a collection of atomic and near-atomic structures of the spliceosome at its different stages has been obtained in the past two years (Figure 1). Together, these structures have shed new light on our understanding of the intricate organisation of the intact spliceosome and splicing mechanism, and provided the structural basis for elucidating the common evolutionary origin between the spliceosome and group II intron (3–5). In addition, structure determination in splicing complexes also helps to ascertain precisely

*To whom correspondence should be addressed. Tel: +86 28 62739162; Email: chengfu.sun@cmc.edu.cn
Correspondence may also be addressed to Xu Jia. Tel: +86 28 62739162; Email: jiaxu@cmc.edu.cn

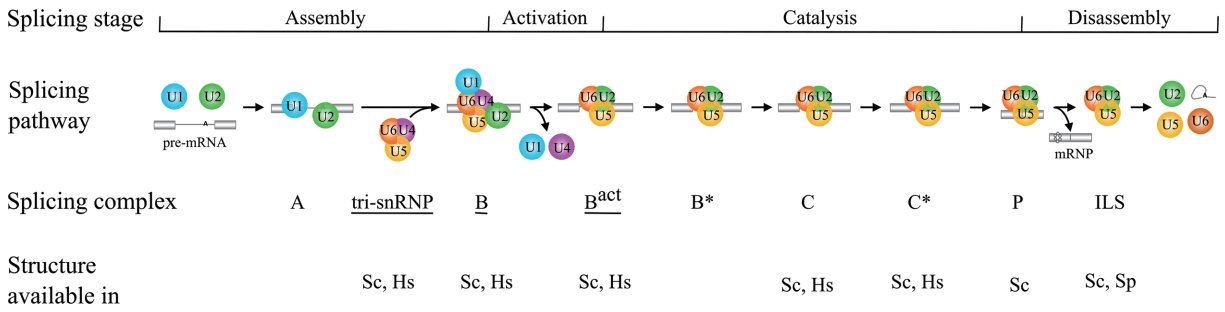

Figure 1. Schematic representation of the splicing pathway. The splicing pathway includes four stages and is executed by eight spliceosomal complexes. The three complexes that are underlined are addressed in this review. A short summary of the spliceosome structures solved to date (February 2018) is listed below. Sc: *Saccharomyces cerevisiae*; Hs: *Homo sapiens*; Sp: *Schizosaccharomyces pombe*.

the different sub-stages of the splicing process as exemplified by the yeast and human tri-snRNP complexes (6–8). Among the four steps of the splicing pathway, spliceosome assembly and activation remain less well understood. Recently, atomic structures of the spliceosomal pre-catalytic B and activated B^{act} complexes, which correspond to stages prior to and after spliceosome activation, have been determined by cryo-EM (9–14). Here, we scrutinise the amino-terminal domain (N-domain) and the Switch loop of Prp8, the largest and most conserved protein in the spliceosome, within these structures, and obtain some new insights regarding the process of spliceosome assembly and activation.

DISCUSSION

Dynamics of the N-domain of Prp8

Prp8 consists of four domains: the N-domain, the Core (also called the Large domain), RNase H-like (RH) and Jab1/MPN (Figure 2A) (4). As the evolutionary counterpart of group II maturase (15), the Core of Prp8 can be further divided into four subdomains: reverse transcriptase (RT) fingers/palm, thumb/X, linker and endonuclease-like (En). Of the four Prp8 domains, the structure of the N-domain has only become available by recent cryo-EM within the intact spliceosome, whereas structures of the other three domains were determined previously by crystallography (16–21). Structural analysis of different cryo-EM structures of spliceosomal complexes showed that, whereas the N-domain binds to U5 snRNA together with Snu114 as a rather rigid functional unit, its position relative to the Core is variable. To date, three distinct conformations of Prp8 between the N-domain and the Core have been observed: open, partially closed and completely closed (Figure 2B) (11). Prior to spliceosome activation, Prp8 adopts a partially closed conformation in the pre-catalytic B complex. However, it changes into the completely closed conformation following activation in the B^{act} complex. This conformation is subsequently well maintained during catalysis and disassembly stages in the C, C*, P and ILS complexes (4,22–25). The open conformation has only been observed in the structure of the human tri-snRNP. Notably, Prp8 in the yeast tri-snRNP structure, in which the Brr2 position is different from that in human, adopts a partially closed conformation similar to that in the pre-catalytic B complex structures. Clearly, there is a tight correlation between the three conformations and these functional states of splicing complexes.

Because the 5′ exon resides in the channel between the N-domain and the Core during catalysis, this location is accordingly called the exon channel (9). Although Prp8 assumes the same partially closed conformation in the structures of both yeast and human pre-catalytic B complexes, the exon channel harbours different RNA molecules in these two complexes (11,12). In the yeast B complex structure, the 5′ end of U6 runs through this channel, whereas in human the 5′ exon is wrapped up this location, arguing that the identified structures of the yeast and human B complexes represent different pre-catalytic states.

In addition, comparison between structures of the pre-catalytic B and activated B^{act} complexes in yeast showed that the RNAs in the exon channel also differ. That is, the 5′ end of U6 in the B complex is replaced by the 5′ exon in the B^{act} complex. The different RNA configurations in these two complexes indicate that there must be a conformational change of Prp8 for toggling of these two molecules during spliceosome activation in yeast. We propose that the partially closed conformation would transiently turn to a more opened conformation for exchanging of the 5′ exon with the 5′ end of U6, and then return to the completely closed conformation during activation in yeast (Figure 2C). In comparison, in human, the positions of the 5′ end of U6 and the 5′ exon in the structure of the pre-catalytic B complex, which are similar to those in B^{act} complexes, are already in place in preparation for catalysis (11,13,14). This suggests that, an equivalent conformation change as is observed in the yeast structures is unlikely to occur in human during spliceosome activation.

Regulation of Prp8 conformation by the Prp38 complex

As mentioned above, Prp8 adopts different conformations within the cryo-EM structures of yeast and human tri-snRNPs. Actually, this conformational difference may be explained by the distinct structural organisation of the complex between these two organisms. In the structure of the human tri-snRNP, hSad1 stably associates with the complex and locks Brr2 in an inactive state by preventing its loading onto the substrate U4 snRNA (6,26). However, Sad1 only weakly interacts with the tri-snRNP in yeast (27). In accordance with this, Sad1 was not present and Brr2 was already loaded onto U4 in the cryo-EM structures of the yeast tri-

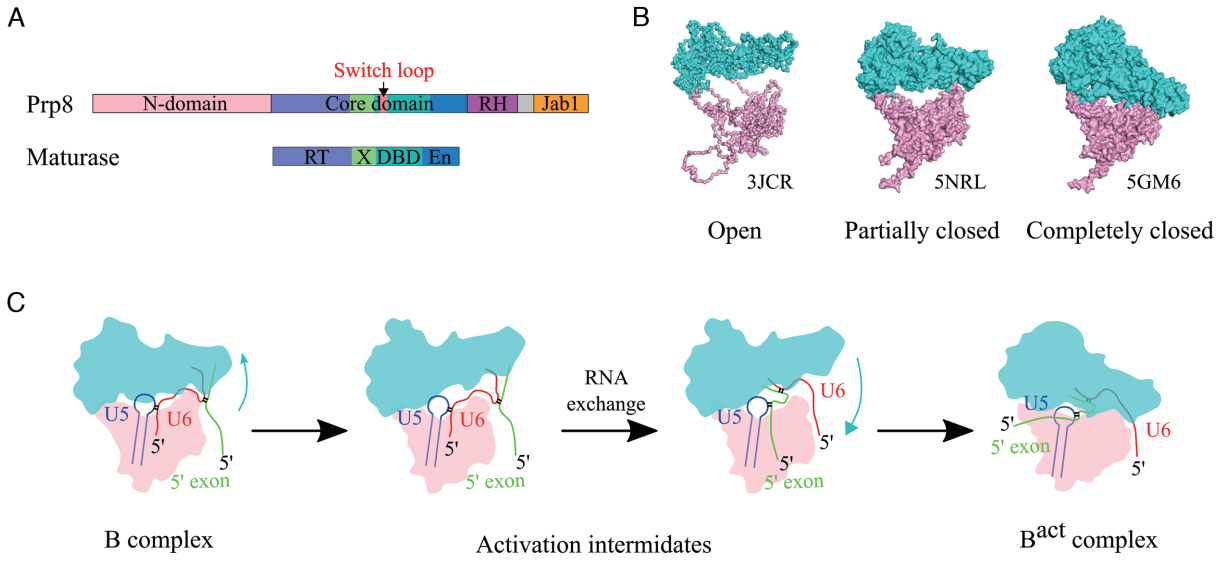

Figure 2. (**A**) Schematic representation of domain architectures of Prp8 and group II maturase. The four domains of Prp8 are labeled and colour-coded. The Core domain of Prp8 and the maturase from *Lactococcus lactics* (50) both contain four subdomains, which are also colour-coded. The location of the Switch loop in Prp8 is indicated. (**B**) Three conformations of Ppr8 between the N-domain (pink) and the Core (cyan). The PDB codes for depiction of the structures are also indicated. For clarity, RH and Jab1 of Prp8 are not shown. (**C**) Proposed conformational changes of Prp8 and RNA toggling between the 5′ exon (green) and the 5′ end of U6 (red) during spliceosome activation in yeast. U5 is also shown and colored in blue.

snRNP (7,8). As the yeast tri-snRNP structure is well maintained in the yeast B complex structure and also resembles the tri-snRNP part in the human B complex structure, it can be inferred that, the state in the human tri-snRNP structure precedes that in the yeast structure during tri-snRNP assembly. Therefore, these two states are accordingly termed tri-snRNP state 1 and 2 (Figure 3). As only a single state has been observed in either yeast or human to date, we consider that state 1 would likely be stable in human but unstable or transient in yeast; whereas state 2 would likely be stable in yeast but unstable or transient in human.

Previously, it was found that the Prp38 complex (composed of Prp38, Snu23 and Spp381/MFAP1) is recruited into the spliceosome as a tri-snRNP component in yeast. In comparison, in human, it enters the spliceosome during B complex assembly as a non-snRNP complex (28). The different incorporation timing of Prp38 complex between yeast and human indicates that this complex may play different roles during tri-snRNP and spliceosome assembly in different organisms (Figure 3).

Considering the presence of the Prp38 complex, which interacts with U4-loaded Brr2 through its Spp381 and Snu23 components, and the lack of Sad1 in the purified yeast tri-snRNP used for cryo-EM structure determination, it is possible that the incorporation of the Prp38 complex would promote the dissociation of Sad1 and accelerate the flipping of Brr2 from state 1 to state 2 during the assembly of a stable yeast tri-snRNP. Alternatively, for human tri-snRNP, the absence of the Prp38 complex make it necessary for hSad1 to hold Brr2 away from its substrate to allow the stable existence of the complex. It would thus be interesting to capture the yeast tri-snRNP in the absence of the Prp38 complex, and to determine the presence of Sad1 and the position of Brr2 in the complex.

Aside from its putative role in tri-snRNP assembly, the Prp38 complex may also account for the distinct Prp8 conformations and RNA content within the exon channel between yeast and human structures during spliceosome assembly. In the structures of both yeast and human pre-catalytic B complexes, the Prp38 complex is located between the N-domain and the En of the Core domain of Prp8, suggesting it would anchor the partially closed conformation of Prp8 (11,12). In yeast, the configuration of the Prp38 complex relative to Prp8 in tri-snRNP was believed to be the same as that in B complex, although its location was not determined in tri-snRNP owning to poor electron density (12). Similar configurations consequently likely account for the same partially closed conformations of Prp8 between these two complexes during spliceosome assembly. This further indicates that the RNA content within the exon channel, the 5′ end of U6, in yeast tri-snRNP, is right locked by the Prp38 complex and remains unchanged after being recruited into the B complex. Conversely, in human, the open conformation of Prp8 in tri-snRNP is converted to the partially closed conformation during spliceosome assembly, consequent to the exchange of U1 and U6 for basepairing to the 5′ splice site catalysed by Prp28, and then is locked by the Prp38 complex which enters simultaneously as a non-snRNP complex. Based on above analysis, we therefore propose that the different configurations of RNA molecules in the exon channels of the yeast and human B complexes, are essentially caused by the different incorporation timing of the Prp38 complex.

The structural organisation difference between yeast and human tri-snRNP cryo-EM structures in addition to the disintegration property upon addition of ATP and the contamination of the spliceosomal B complex in the purified yeast tri-snRNPs used for structure determination (7,8), have recently led some researchers to conclude that the yeast

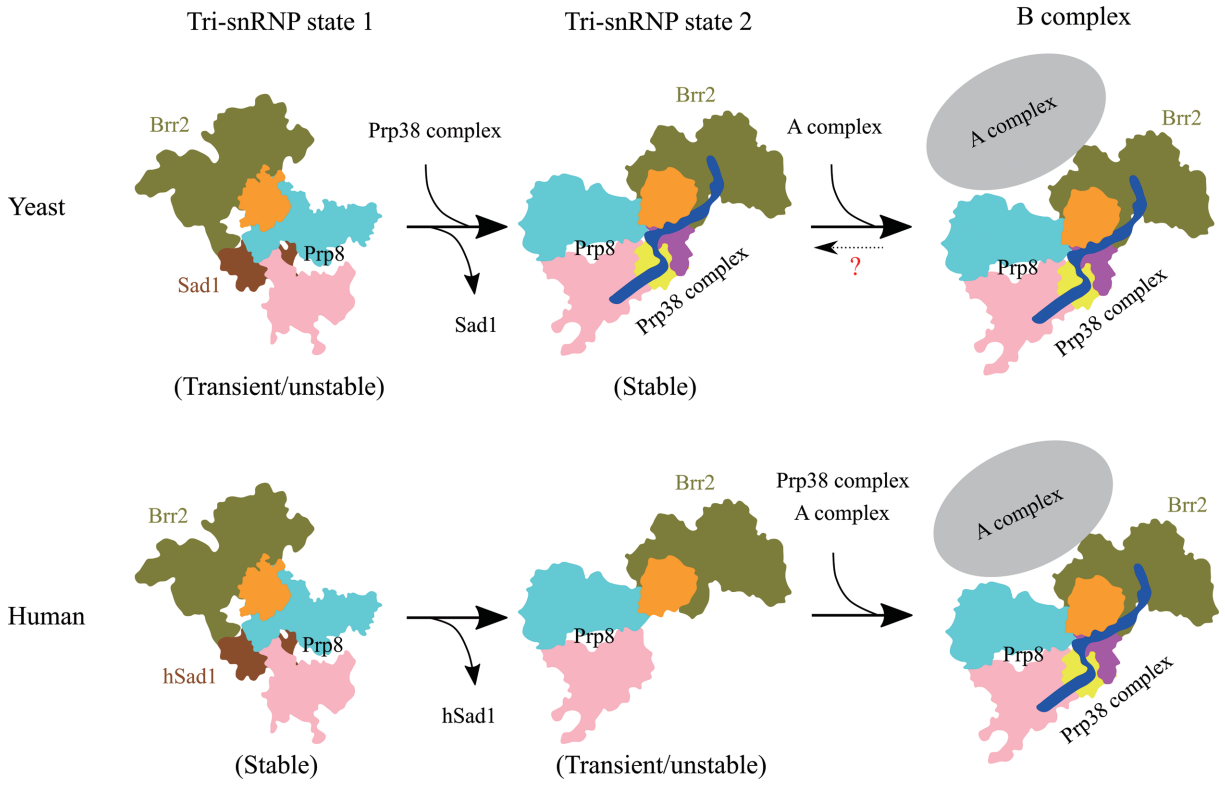

Figure 3. Proposed transition paths from tri-snRNP to the spliceosomal B complex between yeast and human. In yeast tri-snRNP, state 2 is stabilised by the Prp38 complex after Sad1 release; whereas in human tri-snRNP, state 1 is stable. The possibility of dissociation from the B complex to tri-snRNP state 2 in yeast occurring either *in vitro* or *in vivo* cannot be excluded and therefore is indicated with a question mark coloured in red. RH of Prp8 is not shown for clarity and the other three domains are coloured in pink (N-domain), cyan (Core) and orange (Jab1).

tri-snRNP as observed in the cryo-EM structure may derive from dissociated pre-catalytic B complexes and thus do not actually exist in the cell (11,29,30). Although the possibility of such derivation from dissociated endogenous B complex cannot be excluded, the cellular existence of this tri-snRNP should remain undoubted, as this complex has been characterized biochemically and structurally in different laboratories (31–34). Disintegration of the purified yeast tri-snRNP upon addition of ATP is likely caused by loss of factors that maintain the integration of the complex during the purification step (35). Moreover, the contamination of B complexes in the purified yeast tri-snRNP may be due to the different procedure (gel filtration instead of glycerol gradient) used for purification of the complex (8). In fact, the presence of this yeast tri-snRNP could be readily validated by the isolation and characterization of the complex following the *in vivo* depletion of factors that are required for B complex formation.

Functional implication of the Switch loop of Prp8

Another notable feature of Prp8, which was also first observed within the cryo-EM structure of the spliceosome, is the Switch loop (Figure 2A). The Switch loop is a short fragment (residues 1402–1439 in *Saccharomyces cerevisiae*) that stretches out from the linker of the Core domain in Prp8. As shown in Figure 4A, there are two different conformations of the Switch loop (4). One conformation, the tip of the Switch loop pointing towards the intersection of the RT finger/palm, the thumb/X and the N-domain, is observed only in activated and catalytic spliceosomal complexes (B^{act}, C, C* and P) in which the 5′ exon is already loaded in the exon channel of Prp8 (4,22–25). Hence this conformation is termed the active form of the Switch loop. The other conformation, accordingly called the inactive form, in which the Switch loop flips 180° and touches the En of the Core domain, is found in other Prp8-containing complexes (B and ILS, tri-snRNP and Prp8-Aar2 complexes) (4,11,12,21). During spliceosome activation, the Switch loop changes its conformation from the inactive to the active form, and interacts with the 5′ exon together with Cwc21, a B^{act} specific protein. The configuration of the active form of the Switch loop suggests that it plays a role in stabilising the 5′ exon during catalysis.

Structure examination of the pre-catalytic B and activated B^{act} complexes shows that, the Switch loop is tightly regulated during spliceosome activation. In the yeast B complex, the inactive form of the Switch loop is held by an unassigned peptide (12), whereas in human it is stabilised by Snu66 (11). Inspection of the mass spectrometric data of the chemically crosslinked yeast tri-snRNP from the Shi laboratory (8), which clearly contained some B complexes, indicates that the unassigned peptide may presumably derive from the carboxyl-terminal Spp381 (Figure 4B). Overall, these results suggest that the Prp38 complex or Snu66 retains the Switch loop in an inactive form prior to spliceosome activation (Figure 4C). In comparison, in the B^{act}

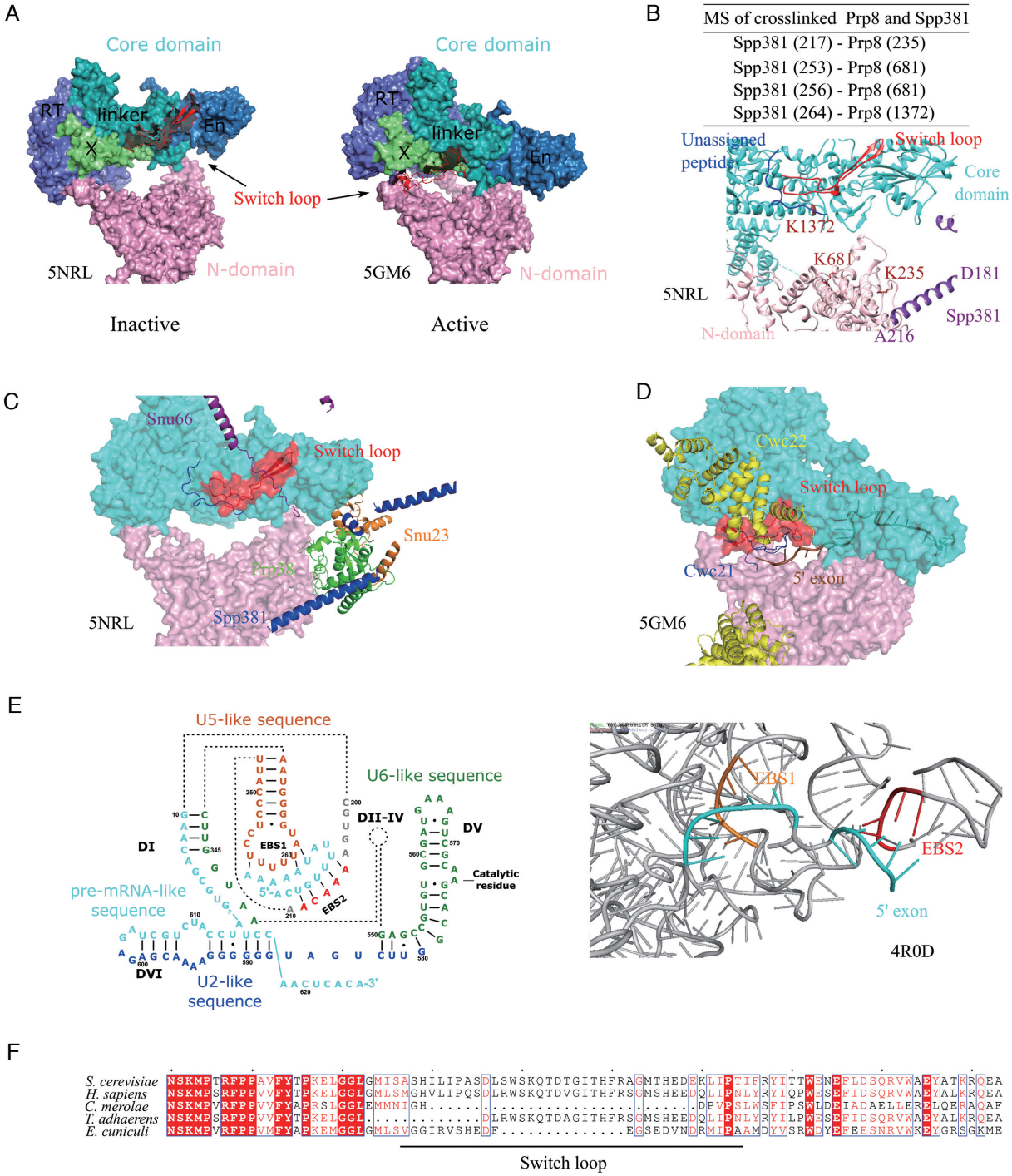

Figure 4. (**A**) Two forms of the Switch loop within Prp8. For clarity, only the N-domain (pink) and subdomains of the Core (coloured as in Figure 2A) of Prp8 are shown. The structures are shown in surface mode except for the Switch loop, which is displayed in cartoon and coloured in red. PDB code for depiction of the structure is also indicated. (**B**) Upper panel, crosslinked residues between Prp8 and C-terminal Spp381 in yeast are listed. Lower panel, location of corresponding crosslinked residues in Prp8 are indicated in the structure and coloured in firebrick. The Switch loop is coloured in red, Spp381 in purple and its putative C-terminus (the unassigned peptide of Chain X in PDB 5NRL) in blue. The PDB code for depiction of the structure is also indicated. (**C**) The Prp38 complex (Spp381 in blue, Prp38 in green and Snu23 in orange) or Snu66 (purple) help to fix the inactive form of the Switch loop in the pre-catalytic B complexes. The PDB code for depiction of the structure is also indicated. (**D**) The active form of the Switch loop is held by Cwc21 (deepblue) and Cwc22 (yellow) after spliceosome activation and during catalysis. 5′ exon is also shown and coloured in brown. Prp8 are depicted in surface while others including the Switch loop in cartoon. The PDB code for depiction of the structure is also indicated. (**E**) Secondary structure of the group II intron (left panel) and corresponding locations of IBS and EBS elements in a crystal structure of group II (PDB 4R0D) (right panel). EBS2 is coloured in red and the exon sequence in cyan. (**F**) Sequence alignment of Prp8 from yeast (*S. cerevisiae*), human (*H. sapiens*), *C. merolae*, *T. adhaerens* and *E. cuniculi* around the Switch loop region.

complex, as well as in subsequent catalytic spliceosomal complexes, the active form of the Switch loop is buttressed by Cwc21 and Cwc22 (Figure 4D) (4). It has been proposed that the active form of the Switch loop is toggled back to the inactive form by the action of Prp22 during the P to ILS transition (22). Although it is unknown how the active form is first established during splicing, its close correlation with the presence of Cwc21 and Cwc22 in spliceosomal complexes strongly suggests that this conformation is formed concurrently with the incorporation of B^{act} specific proteins during spliceosome activation. Because the Ninteen complex (NTC) is required for stable association of U5 and U6 with the spliceosome during spliceosome activation (36), it is conceivable that B^{act} specific proteins and NTC may act in concert to position pre-mRNA and catalytic snRNAs respectively. Considering the different configurations of the Switch loop and its interacting proteins in B and B^{act} complexes, we propose that during spliceosome activation, the Switch loop is first unlocked from its inactive form by removal of the Prp38 complex and Snu66, together with other U4 and U4/U6 proteins, in a process driven by Brr2, then changes into its active form and is subsequently anchored by Cwc21 and Cwc22 when NTC, and possibly also NTC-related (NTR) proteins, enter the spliceosome. In the yeast B complex, the 5′ exon is still outside of the exon channel. Therefore, its loading into the exon channel would be prerequisite for establishment of the active form of the Switch loop during activation.

Sequence comparison between Prp8 and group II maturase showed that the Switch loop or similar sequences is not present in the latter, suggesting that this loop is created during the evolution of the spliceosome. However, the functional implication of the Switch loop in stabilising the 5′ exon during catalysis, renders it a presumable counterpart of another group II intron element, exon-binding site 2 (EBS2) (Figure 4E) (37). EBS sites (EBS1 and EBS2) and their corresponding intron-binding sites (IBS, IBS1 and IBS2), which were identified 30 years ago, function during intron splicing via respective basepairing interactions in group II introns IIA and IIB (38,39). It was initially found that the interaction between loop I of U5 and the 3′ end of 5′ exon in the spliceosome is functionally equivalent to EBS1-IBS1 basepairing (40). However, no counterpart of EBS2-IBS2 interaction has been found in the spliceosome. Here, the presumable function of the active form of the Switch loop allows us to hypothesise that the Switch loop in the spliceosome is equivalent to EBS2 in group II introns. Examples of the replacement of RNA functionality by proteins during evolution has been found previously, such as RNase P (41). The Switch loop may possibly represent another such example during evolution.

Previously, *in vitro* biochemical studies found that loop I of U5 is dispensable for the first catalytic step in yeast and for both steps in human during splicing (42,43). Considering the possibility that the Switch loop functions as an EBS2 element, the dispensability of U5 loop I in splicing would likely be partially compensated by the Switch loop during catalysis. This further indicates that U5 loop I and the Switch loop may have some functional redundancies in positioning the 5′ exon during splicing. Therefore, it may be worthwhile to test this idea by examining the splicing outcome and efficiency after deleting or truncating the Switch loop and mutating the loop I of U5.

However, evidence also exists that apparently counters the presumable function of the Switch loop on the 5′ exon. First, the Switch loop region of *PRP8* gene in *S. cerevisiae* is a hotspot site for transposon insertion of a 69-bp sequence in an *in vitro* study (44). Second, this loop is missing in *Cyanidioschyzon merolae* (*C. merolae*), whose spliceosome is highly streamlined, and partially missing in *Trichoplax adhaerens* (*T. adhaerens*) and *Encephalitozoon cuniculi* (*E. cuniculi*) (Figure 4F). It is likely that the function of the Switch loop in splicing is differentially compromised or streamlined in different organisms during evolution. Nevertheless, experimental dissection of the Switch loop is awaited to understand its authentic mechanism in splicing.

PERSPECTIVES

The recent explosion of high resolution structures of the spliceosome spanning the whole splicing cycle, provides a wealth of new data, as well as new questions regarding this complex splicing machinery. Here, by scrutinising two Prp8 elements, the N-domain and the Switch loop, within structures of the spliceosome both prior to and after activation, we delineated the dynamic organisation and underlying functional significance of these two elements during spliceosome assembly and activation. It is worth noting that our analyses and hypotheses are heavily based on recent cryo-EM structures, which may be influenced by details of sample preparation and structural annotation for determination of these structures, and therefore may not reflect the authentic situation in the cell. Moreover, the splicing process and the spliceosome are more complex than what we have understood, as some spliceosomal complexes or intermediates cannot be properly located within the splicing process (45,46). As argued by Mayerle and Christine Guthrie that (47), the utilization of biochemistry and genetics, in addition to other biophysical approaches such as single-molecule fluorescence resonance energy (smFRET) as have been witnessed in the ribosome field (48) and recently in the splicing field (49), are required for a complete understanding of the mechanism of pre-mRNA splicing. Spliceosome activation generates the catalytic RNA network and sets the stage for the upcoming catalysis during splicing. However, this process is poorly understood compared to others. Detailed investigation of this transition thus requires further biochemical and structural dissection of the process.

FUNDING

National Natural Science Foundation of China [81373454]; Natural Science Foundation of Chengdu Medical College [CYZ17-01]. Funding for open access charge: National Natural Science Foundation of China [81373454]; Natural Science Foundation of Chengdu Medical College [CYZ17-01].
Conflict of interest statement. None declared.

REFERENCES

1. Wahl,M.C., Will,C.L. and Lührmann,R. (2009) The spliceosome: design principles of a dynamic RNP machine. *Cell*, **136**, 701–718.

2. Yan,C., Hang,J., Wan,R., Huang,M., Wong,C.C. and Shi,Y. (2015) Structure of a yeast spliceosome at 3.6-angstrom resolution. *Science*, **349**, 1182–1191.
3. Fica,S.M. and Nagai,K. (2017) Cryo-electron microscopy snapshots of the spliceosome: structural insights into a dynamic ribonucleoprotein machine. *Nat. Struct. Mol. Biol.*, **24**, 791–799.
4. Shi,Y. (2017) Mechanistic insights into precursor messenger RNA splicing by the spliceosome. *Nat. Rev. Mol. Cell. Biol.*, **18**, 655–670.
5. Galej,W.P., Toor,N., Newman,A.J. and Nagai,K. (2018) Molecular mechanism and evolution of nuclear pre-mRNA and group II intron splicing: insights from cryo-electron microscopy structures. *Chem Rev.*, doi:10.1021/acs.chemrev.7b00499.
6. Agafonov,D.E., Kastner,B., Dybkov,O., Hofele,R.V., Liu,W.T., Urlaub,H., Lührmann,R. and Stark,H. (2016) Molecular architecture of the human U4/U6.U5 tri-snRNP. *Science*, **351**, 1416–1420.
7. Nguyen,T.H.D., Galej,W.P., Bai,X.C., Oubridge,C., Newman,A.J., Scheres,S.H.W. and Nagai,K. (2016) Cryo-EM structure of the yeast U4/U6.U5 tri-snRNP at 3.7 A resolution. *Nature*, **530**, 298–302.
8. Wan,R., Yan,C., Bai,R., Wang,L., Huang,M., Wong,C.C. and Shi,Y. (2016) The 3.8 A structure of the U4/U6.U5 tri-snRNP: Insights into spliceosome assembly and catalysis. *Science*, **351**, 466–475.
9. Rauhut,R., Fabrizio,P., Dybkov,O., Hartmuth,K., Pena,V., Chari,A., Kumar,V., Lee,C.T., Urlaub,H., Kastner,B. *et al.* (2016) Molecular architecture of the Saccharomyces cerevisiae activated spliceosome. *Science*, **353**, 1399–1405.
10. Yan,C., Wan,R., Bai,R., Huang,G. and Shi,Y. (2016) Structure of a yeast activated spliceosome at 3.5 A resolution. *Science*, **353**, 904–911.
11. Bertram,K., Agafonov,D.E., Dybkov,O., Haselbach,D., Leelaram,M.N., Will,C.L., Urlaub,H., Kastner,B., Lührmann,R. and Stark,H. (2017) Cryo-EM structure of a pre-catalytic human spliceosome primed for activation. *Cell*, **170**, 701–713.
12. Plaschka,C., Lin,P.C. and Nagai,K. (2017) Structure of a pre-catalytic spliceosome. *Nature*, **546**, 617–621.
13. Haselbach,D., Komarov,I., Agafonov,D.E., Hartmuth,K., Graf,B., Dybkov,O., Urlaub,H., Kastner,B., Lührmann,R. and Stark,H. (2018) Structure and conformational dynamics of the human spliceosomal B^{act} complex. *Cell*, **172**, 454–464.
14. Zhang,X., Yan,C., Zhan,X., Li,L., Lei,J. and Shi,Y. (2018) Structure of the human activated spliceosome in three conformational states. *Cell Res.*, **28**, 307–322.
15. Zhao,C. and Pyle,A.M. (2017) Structural insights into the mechanism of group II intron splicing. *Trends Biochem. Sci.*, **42**, 470–482.
16. Pena,V., Liu,S., Bujnicki,J.M., Lührmann,R. and Wahl,M.C. (2007) Structure of a multipartite protein-protein interaction domain in splicing factor prp8 and its link to retinitis pigmentosa. *Mol. Cell*, **25**, 615–624.
17. Zhang,L., Shen,J., Guarnieri,M.T., Heroux,A., Yang,K. and Zhao,R. (2007) Crystal structure of the C-terminal domain of splicing factor Prp8 carrying retinitis pigmentosa mutants. *Protein Sci.*, **16**, 1024–1031.
18. Pena,V., Rozov,A., Fabrizio,P., Lührmann,R. and Wahl,M.C. (2008) Structure and function of an RNase H domain at the heart of the spliceosome. *EMBO J.*, **27**, 2929–2940.
19. Ritchie,D.B., Schellenberg,M.J., Gesner,E.M., Raithatha,S.A., Stuart,D.T. and Macmillan,A.M. (2008) Structural elucidation of a PRP8 core domain from the heart of the spliceosome. *Nat. Struct. Mol. Biol.*, **15**, 1199–1205.
20. Yang,K., Zhang,L., Xu,T., Heroux,A. and Zhao,R. (2008) Crystal structure of the beta-finger domain of Prp8 reveals analogy to ribosomal proteins. *Proc. Natl. Acad. Sci. U.S.A.*, **105**, 13817–13822.
21. Galej,W.P., Oubridge,C., Newman,A.J. and Nagai,K. (2013) Crystal structure of Prp8 reveals active site cavity of the spliceosome. *Nature*, **493**, 638–643.
22. Bai,R., Yan,C., Wan,R., Lei,J. and Shi,Y. (2017) Structure of the post-catalytic Spliceosome from *Saccharomyces cerevisiae*. *Cell*, **171**, 1589–1598.
23. Liu,S., Li,X., Zhang,L., Jiang,J., Hill,R.C., Cui,Y., Hansen,K.C., Zhou,Z.H. and Zhao,R. (2017) Structure of the yeast spliceosomal postcatalytic P complex. *Science*, **358**, 1278–1283.
24. Wilkinson,M.E., Fica,S.M., Galej,W.P., Norman,C.M., Newman,A.J. and Nagai,K. (2017) Postcatalytic spliceosome structure reveals mechanism of 3′-splice site selection. *Science*, **358**, 1283–1288.
25. Zhan,X., Yan,C., Zhang,X., Lei,J. and Shi,Y. (2018) Structure of a human catalytic step I spliceosome. *Science*, **359**, 537–545.
26. Makarova,O.V., Makarov,E.M. and Lührmann,R. (2001) The 65 and 110 kDa SR-related proteins of the U4/U6.U5 tri-snRNP are essential for the assembly of mature spliceosomes. *EMBO J.*, **20**, 2553–2563.
27. Huang,Y.H., Chung,C.S., Kao,D.I., Kao,T.C. and Cheng,S.C. (2014) Sad1 counteracts Brr2-mediated dissociation of U4/U6.U5 in tri-snRNP homeostasis. *Mol. Cell. Biol.*, **34**, 210–220.
28. Ulrich,A.K. and Wahl,M.C. (2017) Human MFAP1 is a cryptic ortholog of the Saccharomyces cerevisiae Spp381 splicing factor. *BMC Evol. Biol.*, **17**, 91.
29. Absmeier,E., Wollenhaupt,J., Mozaffari-Jovin,S., Becke,C., Lee,C.T., Preussner,M., Heyd,F., Urlaub,H., Lührmann,R., Santos,K.F. *et al.* (2015) The large N-terminal region of the Brr2 RNA helicase guides productive spliceosome activation. *Genes Dev.*, **29**, 2576–2587.
30. Absmeier,E., Santos,K.F. and Wahl,M.C. (2016) Functions and regulation of the Brr2 RNA helicase during splicing. *Cell Cycle*, **15**, 3362–3377.
31. Gottschalk,A., Neubauer,G., Banroques,J., Mann,M., Lührmann,R. and Fabrizio,P. (1999) Identification by mass spectrometry and functional analysis of novel proteins of the yeast [U4/U6.U5] tri-snRNP. *EMBO J.*, **18**, 4535–4548.
32. Stevens,S.W. and Abelson,J. (1999) Purification of the yeast U4/U6.U5 small nuclear ribonucleoprotein particle and identification of its proteins. *Proc. Natl. Acad. Sci. U.S.A.*, **96**, 7226–7231.
33. Mougin,A., Gottschalk,A., Fabrizio,P., Lührmann,R. and Branlant,C. (2002) Direct probing of RNA structure and RNA-protein interactions in purified HeLa cell's and yeast spliceosomal U4/U6.U5 tri-snRNP particles. *J. Mol. Biol.*, **317**, 631–649.
34. Häcker,I., Sander,B., Golas,M.M., Wolf,E., Karagöz,E., Kastner,B., Stark,H., Fabrizio,P. and Lührmann,R. (2008) Localization of Prp8, Brr2, Snu114 and U4/U6 proteins in the yeast tri-snRNP by electron microscopy. *Nat. Struct. Mol. Biol.*, **15**, 1206–1212.
35. Stevens,S.W., Barta,I., Ge,H.Y., Moore,R.E., Young,M.K., Lee,T.D. and Abelson,J. (2001) Biochemical and genetic analyses of the U5, U6, and U4/U6 x U5 small nuclear ribonucleoproteins from Saccharomyces cerevisiae. *RNA*, **7**, 1543–1553.
36. Chan,S.P., Kao,D.I., Tsai,W.Y. and Cheng,S.C. (2003) The Prp19p-associated complex in spliceosome activation. *Science*, **302**, 279–282.
37. Robart,A.R., Chan,R.T., Peters,J.K., Rajashankar,K.R. and Toor,N. (2014) Crystal structure of a eukaryotic group II intron lariat. *Nature*, **514**, 193–197.
38. Jacquier,A. and Michel,F. (1987) Multiple exon-binding sites in class II self-splicing introns. *Cell*, **50**, 17–29.
39. Pyle,A.M. (2016) Group II Intron Self-Splicing. *Annu. Rev. Biophys.*, **45**, 183–205.
40. Hetzer,M., Wurzer,G., Schweyen,R.J. and Mueller,M.W. (1997) Trans-activation of group II intron splicing by nuclear U5 snRNA. *Nature*, **386**, 417–420.
41. Gobert,A., Gutmann,B., Taschner,A., Gössringer,M., Holzmann,J., Hartmann,R.K., Rossmanith,W. and Giegé,P. (2010) A single Arabidopsis organellar protein has RNase P activity. *Nat. Struct. Mol. Biol.*, **17**, 740–744.
42. O'Keefe,R.T., Norman,C. and Newman,A.J. (1996) The invariant U5 snRNA loop 1 sequence is dispensable for the first catalytic step of pre-mRNA splicing in yeast. *Cell*, **86**, 679–689.
43. Ségault,V., Will,C.L., Polycarpou-Schwarz,M., Mattaj,I.W., Branlant,C. and Lührmann,R. (1999) Conserved loop I of U5 small nuclear RNA is dispensable for both catal.ytic steps of pre-mRNA splicing in HeLa nuclear extracts. *Mol. Cell. Biol.*, **19**, 2782–2790.
44. Turner,I.A., Norman,C.M., Churcher,M.J. and Newman,A.J. (2006) Dissection of Prp8 protein defines multiple interactions with crucial RNA sequences in the catalytic core of the spliceosome. *RNA*, **12**, 375–386.
45. Ast,G. and Weiner,A.M. (1996) A U1/U4/U5 snRNP complex induced by a 2′-O-methyl-oligoribonucleotide complementary to U5 snRNA. *Science*, **272**, 881–884.
46. Chen,Z., Gui,B., Zhang,Y., Xie,G., Li,W., Liu,S., Xu,B., Wu,C., He,L., Yang,J. *et al.* (2017) Identification of a 35S U4/U6.U5 tri-small nuclear ribonucleoprotein (tri-snRNP) complex intermediate in spliceosome assembly. *J. Biol. Chem.*, **292**, 18113–18128.
47. Mayerle,M. and Guthrie,C. (2017) Genetics and biochemistry remain essential in the structural era of the spliceosome. *Methods*, **125**, 3–9.

48. Perez,C.E. and Gonzalez,R.L. Jr (2011) In vitro and in vivo single-molecule fluorescence imaging of ribosome-catalyzed protein synthesis. *Curr. Opin. Chem. Biol.*, **15**, 853–863.
49. Blanco,M.R., Martin,J.S., Kahlscheuer,M.L., Krishnan,R., Abelson,J., Laederach,A. and Walter,N.G. (2015) Single molecule cluster analysis dissects splicing pathway conformational dynamics. *Nat. Methods*, **12**, 1077–1084.
50. Qu,G., Kaushal,P.S., Wang,J., Shigematsu,H., Piazza,C.L., Agrawal,R.K., Belfort,M. and Wang,H.W. (2016) Structure of a group II intron in complex with its reverse transcriptase. *Nat. Struct. Mol. Biol.*, **23**, 549–557.